CHINESE JOURNAL OF MECHANICAL ENGINEERING
Vol. 27, No. 2, 2014

DOI: 10.3901/CJME.2014.02.348, available online at www.springerlink.com; www.cjmenet.com; www.cjmenet.com.cn

Novel Application-oriented Transient Fuel Model of a Port Fuel Injection S. I. Engine

WANG Cunlei *, ZHANG Jianlong, and YIN Chengliang

National Engineering Laboratory for Automotive Electronic Control Technology, Shanghai Jiao Tong University, Shanghai 200240, China

Received June 20, 2013; revised December 9, 2013; accepted December 13, 2013

Abstract: Most researches on transient fuel control of port fuel injection S.I. engine are carried out from the perspective of advanced mathematical theories. When it comes to practical control, there exist many limitations although they are more intelligent. In order to overcome the fuel wetting effect of PFI engine, the application-oriented transient fuel control is studied by analyzing the key parameters which are closely related with the engine transient characteristics. Both validity and simplicity are taken into consideration. Based on the fuel wall-wetting theory and popular fuel compensation strategy, short-term transient fuel(STF) and long-term transient fuel(LTF), as well as their individual decay approaches, are introduced. STF is to compensate the drastic fuel film loss caused by sudden throttle change, while the function of LTF is to compensate the fuel film loss by manifold air pressure(p) fluctuation. Each of them has their respective pros and cons. The engine fuel mass and air mass are also calculated for air-fuel ratio(AFR) according to ideal gas state equation and empirical equations. The vehicle acceleration test is designed for model validation. The engine experiences several mild and heavy accelerations corresponding to the gear change during vehicle acceleration. STF and LTF control are triggered reliably. The engine transient fuel control simulation adopts the same inputs as the test to ensure consistency. The logged test data are used to check the model output. The results show that the maximum fuel pulse width(FPW) error reaches 2 ms, and it only occurs under engine heavy acceleration condition. The average FPW error is 0.57 ms. The results of simulation and test are close overall, which indicates the accuracy of steady and transient fuel. The proposed research provides an efficient approach not only suitable for practical engineering application, but also for AFR prediction, fuel consumption calculation, and further studies on emission control.

Keywords: engine, strategy, transient, fuel, model

1 Introduction

At present, the three-way catalyst(TWC) has been the requisite equipment for gasoline engine along with the increasingly strict emission regulation. TWC only keeps high conversion efficiency when air-fuel ratio(AFR) falls within the narrow band of 14.7±0.147[1]. TWC can purify the most pollutant of steady state whereas the conversion efficiency of transient state cannot be ensured. The engine transients should be targeted at emission control while attention must be paid to fuel consumption at engine steady state[2]. For either regulation cycle test or real-road driving, engine transients occur frequently. The engine will operate at low emission standard if the AFR excursion is under control. For S.I. engine, the throttle is an actuator for air control, and the fuel delivery is determined by air mass flow. Thus the AFR control means fuel control to some extent.

The wall-wetting effect cannot be avoided for port fuel injection engine. The deposit-evaporation balance will be destroyed at engine transients. Thus the transient fuel is critical in order to meet the demand of vehicle drivability and transient AFR. The reasons of necessity of transient fuel are listed as follows.

(1) Dead band time between manifold air pressure(p) sensor and intake valve. There is a dead band time between p and actual load when intake valve closes. The air pressure when intake valve closes cannot be reflected with the measured p.

(2) Error of dynamic load signal. Under dynamic circumstances, the p sensor fails to reflect the actual in-cylinder air mass flow.

(3) Wall wetting effect. For port fuel injection engine, the fuel is injected into manifold and gets into cylinder with air flow. The injected fuel will not fully be aspirated into cylinder. There is some fuel adhered to inner wall of manifold to form the fuel film.

The deposit percentage is related with injected fuel, air flow rate and inner wall temperature[3]. The deposit fuel and the evaporated fuel achieve dynamic balance at engine steady state. The balance will be destroyed at transients.

(4) Emission control before oxygen sensor and TWC activation. Most emissions are generated at cold start and transients[4].TANG X G[5] proposed an approach to estimate the instantaneous AFR and uses the estimation as a

* Corresponding author. E-mail: clwang@sjtu.edu.cn
This project is supported by the Fund of US-China Collaboration on Cutting-edge Technology Development of Electric Vehicle, Ministry of Science and Technology of China(Grant No. 2010DFA72760-305)

feedback signal to control AFR during cold transients before oxygen sensor activation. Besides oxygen sensor, it also takes some time for TWC to activate after engine cold start. During this time interval, combining with excellent transient fuel control, the coordination of engine and motor helps to reduce engine transient emissions[6] of hybrid electric vehicles.

In recent studies, some researchers focus on the fuel film mechanism theoretical study[7–9]; others attach importance to advanced mathematic method to regulate the AFR[10–11]. Feed-forward control strategy[12–13], adapt algorithm[14], predictive algorithm[15], neural network[16–20], fuzzy control[21], as well as their combination[22], are commonly used. The achievements mentioned above are comprehensive and penetrating. However, complicated mathematical methods are seldom applied in practical controllers and mass-product vehicles because of limitation of flexibility and simplicity. Otherwise the calculation capacity and memory of microprocessor will be reduced or wasted.

There are also researchers who lay emphasis on air-fuel ratio control from experiment perspective and lots of advanced apparatus play an important role in the study [23–25]. ROBERT calculated the cycle-by-cycle AFR during transient engine operation using fast response CO and CO_2 sensors[26]. Many researchers studied the influence of some key parameters to transient AFR[23, 27–28].

In this research, we proposed an application-oriented transient fuel control strategy with the consideration of fast and slow change of engine working condition. The strategy is based on the popular x-τ theoretical model[29–30]. The compensated fuel can be divided into short-term fuel(STF) and long-term fuel(LTF). The objective of the strategy is to regulate the AFR within reasonable band at engine acceleration without the expense of drivability.

The transient fuel control strategy is described in detail in section 2; then in section 3, the model specification is presented, which includes models of air mass, steady fuel and transient fuel control. Consequently, the model is validated via engine acceleration test in section 4, followed by discussions and conclusions.

2 Engine Transient Fuel and Air Strategy

The fuel film tends to evaporate at low p. When the throttle opens suddenly at acceleration, the increased p thickens the deposit fuel film. It takes some time for the deposited fuel to evaporate. So the actual in-cylinder fuel is inadequate and the mixture gets lean. Thus extra fuel is delivered to thicken the mixture. On the other hand, the engine works at high speed at the instant of throttle quick close because of inertia. p decreases drastically and the fuel film is pumped into cylinder. Thus fuel delivery is shortened in case of forming over-rich mixture. Hendricks proposed the fuel evaporation model and transient fuel film compensation model[3], which make in-cylinder fuel equal to desired fuel. The in-cylinder mixture maintains stoichiometric AFR theoretically.

In this paper, the fuel film compensation model is "translated" into two parts, named STF and LTF. STF is to compensate the drastic fuel film change caused by sudden throttle change; the function of LTF is to compensate the fuel film loss by p fluctuation. STF lasts longer than STF and it decays to zero until the fuel film regains dynamic balance. Fig. 1 shows the control scheme of AFR model.

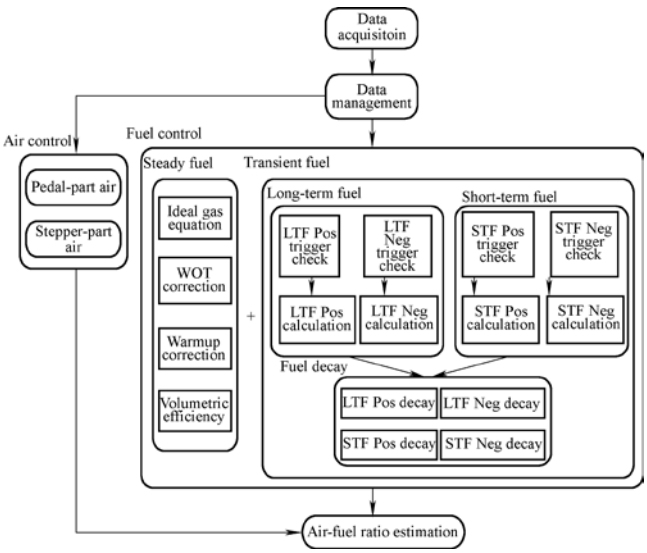

Fig. 1. Control scheme of AFR model

This model can be roughly divided into five parts: data acquisition, data management, air path, fuel path and AFR estimation. The raw acquisition includes signal types of analog, digital, resistor and interrupt event. They are not available unless is managed with reasonable rules(noise elimination, limitation, data type transition, and so on). The main strategy consists of air path and fuel path. The content of air path includes calculation of throttle position(θ) and air mass flow. The throttle opening is composed of two parts corresponding to pedal(pedal-part) and stepping motor(stepper-part).The air mass flow is calculated with p, engine speed(n_e) and throttle position. The fuel path includes parts of steady fuel and transient fuel. The steady fuel is determined on the basis of ideal gas equation. The ideal fuel should be corrected by volumetric efficiency(η_v) to present the in-cylinder fuel. Considering the coolant temperature(T_c) and catalyst protection at throttle wide open(WOT), the corrections of warm-up and WOT fuel are introduced. The transient fuel is integrated into fuel calculation based on engine state management. It can be regarded as a correction to steady fuel. Either STF or LTF compensation applies the same procedure: the program firstly checks if the trigger condition is met. If so, the initial value of STF(or LTF) will be calculated. This value will be

transferred to fuel decay model. The transient fuel shrinks step by step. The shrinking rate of transient fuel is described with the positive and negative decay coefficient corresponding to STF and LTF. With the air mass and fuel mass of each time step, the AFR is determined.

Fig. 2 shows the STF control strategy. Necessary data should be calculated in advance for STF trigger judgment. These data include predicted $p(p_p)$ and its filter coefficient, throttle change rate(d_{TPS}) trigger threshold and basic STF. STF is closely related with d_{TPS}. The p of target engine working point cannot be measured accurately because of air flow hysteresis. It needs to be predicted. d_{TPS} acts as one of the trigger indicators of STF. The other one, named Δp_p, is defined as the difference between p_p and its filtered value. If either the d_{TPS} or Δp_p exceeds their respective threshold, STF is triggered. There are two corrections resulting from n_e and intake air temperature(T_i). The former is used for engine quick speed-up. The latter is used to regulate the fuel film at various T_i. Whether STF Pos or STF Neg will be triggered is determined by the sign of difference of basic LTF(Δt_{sb}) between original and target engine working point. STF is forbidden when the engine operates at STALL or CRANK mode.

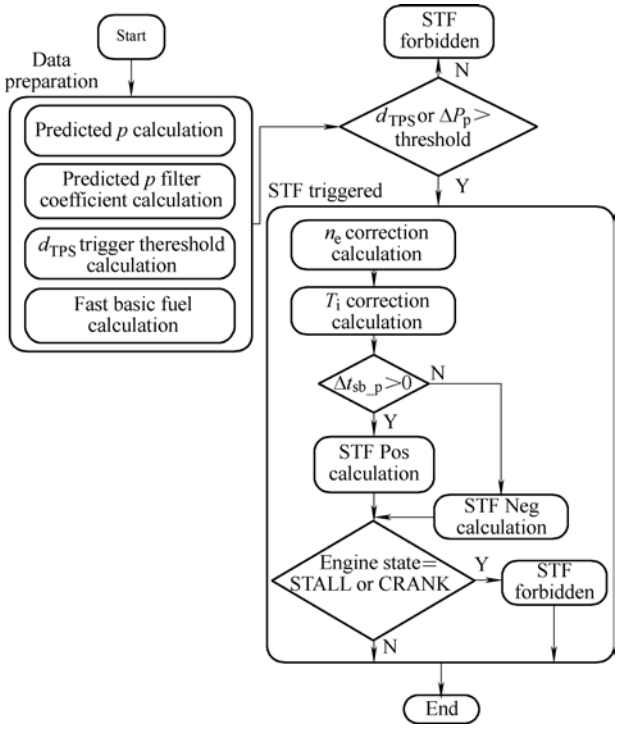

Fig. 2. STF control strategy

Fig. 3 shows the LTF control strategy. STF may be triggered by d_p, or along with STF. If either of the conditions is met, the n_e correction, T_i correction, basic LTF, d_{TPS} and d_p are calculated. Whether LTF Pos or LTF Neg will be triggered is determined by the sign of difference of basic LTF(Δt_{lb}) between the original and the target engine working point. STF is forbidden when the engine operates at STALL or CRANK mode.

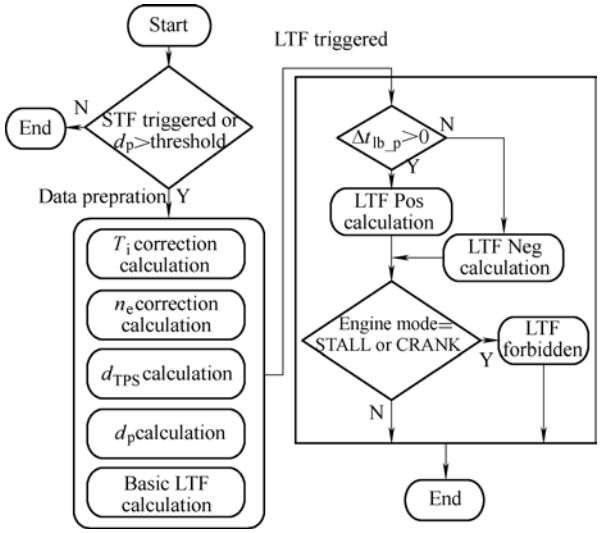

Fig. 3. LTF control strategy

The transient fuel decay coefficients have great influence on emissions. They are roughly calibrated and drivability-oriented firstly, and then they are precisely calibrated on chassis dynamometer. The emissions are tested under specific driving cycle. The transient AFR must be controlled within target band. Excess fuel or over-slow decay leads to much HC and CO emissions, otherwise the NO_x emission will deteriorate. The driving cycle covers almost all the engine working points of universal characteristic. Nearly all accelerations will trigger transient fuel. The fuel decay determines the compensated fuel trace and real-time AFR. Fig. 4 shows the overview of transient fuel decay. There are four types of transient fuel decay: positive STF(STF Pos), negative STF(STF Neg), positive LTF(LTF Pos) and negative LTF(LTF Neg). Their control complies with the same decay procedure. The upper subplot is the desired decay trace. It must be discretized for the sake of practical application. The basic transient fuel is the initial value which comes from the STF(or LTF) control model. The decay process is characterized by control period and decay coefficient.

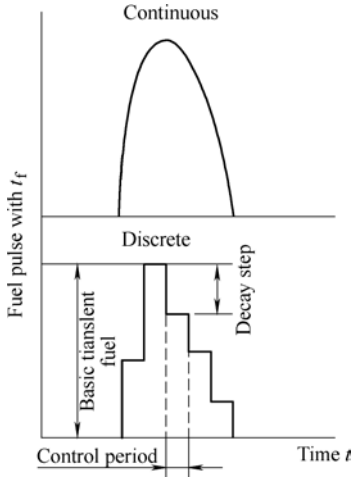

Fig. 4. Transient fuel decay overview

3 Model Specification

The AFR model is established to specify the transient fuel strategy. It is composed of models of fuel path and air path. Detailed fuel control at the steady and transient state is discussed in fuel path model. The air path model takes the charge of air mass flow calculation.

3.1 Fuel path

Fuel pulse width(FPW) calculation contains four parts: basic steady fuel, steady fuel correction, battery voltage(V_b) fuel correction and transient fuel. There are four main engine states: STALL, CRANK, IDLE and RUN. The transient fuel only exists at IDLE and RUN mode even if other transient conditions are met. The steady fuel is the basic injected fuel at IDLE and RUN mode when the engine runs stably.

3.1.1 Steady fuel

(1) Basic steady fuel calculation

The steady fuel is open-loop controlled. The speed-density principle is an indirect method which determines the manifold absolute pressure and temperature. The necessary signals include n_e, p, T_i. Other information such as cylinder working volume(V_h), η_v and gas constant R must be introduced in advance.

The air charge density of manifold can be depicted as

$$\rho_m = p/(R \cdot T_i), \tag{1}$$

where ρ_m—Manifold air density,
p—Manifold air pressure,
R—Ideal gas constant,
T_i—Intake air temperature.

The gasoline engine is not an ideal gas pump，so the air charge loss takes place at the end of intake stroke. The air charge density experiences some change because of overlap of intake and exhaust valve, and it can be expressed as

$$\rho_c = \eta_v / \rho_m , \tag{2}$$

where ρ_c—Intake air density of cylinder.

So the cycle air flow rate can be depicted as

$$q_a = \rho_c V_h = \eta_v \rho_m V_h = \eta_v V_h p/(RT_i) = C\eta_v p/T_i, \tag{3}$$

where q_a—Cycle air flow rate.

V_h is the cylinder working volume and V_h/R can be integrated within one constant C. The cycle fuel flow rate can be calculated through q_a:

$$q_f = (1/A_F)\, q_a, \tag{4}$$

where q_f—Cycle fuel flow rate,
A_F—Stoichiometric AFR.

According to ideal state gas equation and considering the real gas, the coefficient η_i is introduced, which is composed by T_i correction and constant C. The ideal cycle cylinder air charge can be depicted as

$$m'_{cyc} = \eta_i p V_h T_i, \tag{5}$$

where m'_{cyc}—Ideal cycle cylinder air charge mass.

p complies with the equation as

$$V_{out} = V_{ref}(0.008\,095p - 0.000\,952), \tag{6}$$

where V_{ref} is the sensor reference voltage and it is usually $5\ V \pm 0.25\ V$. V_{out} is the output voltage of sensor signal. The p must be digitized into 8-bit signal for the utilization of FPW calculation. Combining Eq. (5) with η_v, the actual cycle air charge into cylinder is

$$m_{cyc} = m'_{cyc} \times \eta_v, \tag{7}$$

where m_{cyc}—Actual cycle cylinder air charge mass.

The fuel calculation is simplified as a function of n_e and p[31]. In this paper, we separate this function as individual calibration data, that is, η_v. η_v is a complex parameter which is at least related with n_e, valve timing, manifold design, EGR, exhaust pressure, and crankcase ventilation. It is determined through engine bench test because it cannot be calculated exactly. So η_v is depicted as a function versus p and n_e, and stored in ECU memory. According to the definition of AFR, the cycle fuel flow rate equals $m_{cyc}/14.7$. Combining Eq. (5) with Eq. (7), the basic fuel pulse is determined by

$$t_s = m_s/q = m_{cyc}/(14.7q) = \eta_i\, \eta_v\, pV_h/(14.7qT_i), \tag{8}$$

where t_s—Steady fuel pulse width,
m_s—Steady fuel mass,
q—Injector flow rate coefficient.

(2) Steady fuel correction. The steady fuel correction comes from warm-up and WOT mode. The warm-up fuel is targeted at engine's quick heating for the sake of fine fuel film evaporation and oil lubrication. It is influenced by T_c and p. The WOT fuel is added to the basic steady fuel in order to meet the power demand and catalyst protection at WOT. It is calibrated according to θ and n_e on engine bench.

(3) Transient fuel. The transient fuel only exists at IDLE and RUN mode. The transient fuel is added to the basic fuel once the corresponding conditions are met. It will be introduced in detail in the following sections.

(4) V_b fuel compensation. Over-low voltage will prolong the injector needle movement. The effective fuel is reduced. So the V_b fuel compensation is necessary to ensure the actual injected fuel.

The run mode fuel is determined by

$$t_f = t_s(1+k_w)k_{WOT}+t_b+t_t, \quad (9)$$

where t_f—Fuel pulse width of engine RUN mode,
k_w—Fuel enrichment coefficient for warm-up,
k_{WOT}—Fuel enrichment coefficient at WOT,
t_b—Fuel compensation of battery voltage,
t_t—Transient fuel pulse width.

3.1.2 *Transient fuel*

3.1.2.1 *Short-term fuel*

STF is influenced by p_p and d_{TPS}. When the throttle is wide open, p of target working point cannot be acquired because of air flow hysteresis. p of target working point needs to be predicted. The d_{TPS} and p_p are calculated according to Eqs. (10) and (11) respectively:

$$d_{TPS}=(\theta-\theta_{prev})/\Delta t_{STF}, \quad (10)$$

where d_{TPS}—Chang rate of throttle,
θ—Throttle position,
θ_{prev}—Throttle position of previous step.

$$p_p=\begin{cases}\min(p_{pb}+k_{dTPS}d_{TPS}, p_a), & d_{TPS}>0,\\ \max(p_{pb}-k_{dTPS}d_{TPS}, 0), & d_{TPS}<0,\end{cases} \quad (11)$$

where Δt_{STF}—STF control period,
p_p—Predicted manifold air pressure,
p_{pb}—Manifold air pressure of calibration point,
d_{TPS}—Change rate of throttle,
k_{dTPS}—Coefficient influenced by d_{TPS},
p_a—Ambient air pressure.

p_p is obtained on bench test. It is the steady p of calibrated engine working point. d_{TPS} and p_p influence the basic STF directly. The difference between p_p and its filtered value is used as the calibration point. Once d_{TPS} or the difference between p_p and its filtered value exceeds their respective threshold, STF Pos is triggered, otherwise STF Pos is forbidden. As for STF Neg, its trigger indicator is the d_{TPS}. If d_{TPS} is less than the calibration value(d_{TPS} is negative), STF Neg is triggered. Besides that d_{TPS} takes part in p_p calculation, it also acts as STF trigger. The wider the throttle is, the higher the trigger threshold is. The p_p filter coefficient is selected reasonably. If the d_{TPS} trigger threshold or the p_p filter coefficient is set too low, STF is triggered too sensitively and leads to much emission. On the other hand, if d_{TPS} trigger threshold or the p_p filter coefficient is set too high, STF is hard to trigger. The engine will speed up slowly. The basic STF is influenced by T_c and p. STF Pos is the sum of STF Pos filtered value of the last calculation step and the change part. The change part is the LTF fuel difference of origin and target working point with correction of n_e and T_i. The T_i correction k_i is to overcome the air mass change resulting from air density. The n_e correction k_n is to supply desired fuel for engine speed-up. There is an extra fuel correction for STF Neg, named k_d. t_{sp_rt} (or t_{sn_rt}) is the real-time subpart of FPW and it is also one of the inputs of fuel decay model. t_{sp_f} (or t_{sn_f}) is one of the outputs of transient fuel decay model. It is used as feedback and takes part in the LTF Pos initial value calculation. t_{sp_rt} and t_{sn_rt} are determined by Eqs. (12) and (13):

$$t_{sprt}=t_{sp\_f}+(t_{sb\_t}-t_{sb\_o})\,k_n\,k_i, \quad (12)$$

$$t_{sn\_rt}=t_{sn\_f}+(t_{sb\_t}-t_{sb\_o})\;k_n\;k_i\;k_d, \quad (13)$$

where t_{sp_rt}—Real-time pulse width of positive STF,
t_{sp_f}—Filtered pulse width of positive STF,
t_{sb_t}—Basic initial pulse width of target working point of STF,
t_{sb_o}—Basic initial pulse width of original working point of STF,
k_n—Coefficient influenced by n_e,
k_i—Coefficient influenced by T_i,
t_{sn_rt}—Real-time pulse width of negative STF,
t_{sn_f}—Filtered pulse width of negative STF,
k_d—Special coefficient for throttle release.

3.1.2.2 *Long-term fuel*

Based on the principle difference between STF and LTF, the LTF control has its individual control period. There are two entrances to LTF control: STF-pilot trigger and d_p trigger. If STF is triggered, LTF definitely follows it. Compared to STF, LTF lasts longer. It is used to compensate mild p fluctuation and avoid over-lean mixture which is caused by unbalanced fuel film deposit and evaporation.

The controller will first check if STF is triggered. If so, several data, such as T_i correction coefficient, n_e correction coefficient, d_{TPS}, d_p and basic LTF will be calculated in advance. The d_p calculation is defined as the difference between p and filtered p within LTF control period, which is shown in Eq. (14):

$$d_p=(p-p_f)/\Delta t_{LTF}, \quad (14)$$

where d_p—Change rate of manifold air pressure,
p_f—Filtered manifold air pressure,
Δt_{LTF}—LTF control period.

$$p_f=\begin{cases}p_{f\_p}+(p-p_{f\_p})k_p, & p>p_{f\_p},\\ p_{f\_p}-(p_{f\_p}-p)k_p, & p\leqslant p_{f\_p},\end{cases} \quad (15)$$

where p_{f_p}—Filtered manifold air pressure of last step,
k_p—Manifold air pressure filter coefficient.

The filtered p(Eq. (15)) represents the hysteresis of air flow and shows the tendency to the immediate p. The basic LTF is determined by immediate p and T_c. The real-time LTF fuel is determined by Eqs. (16) and (17). For LTF Pos, it traces the increment of the difference between the basic

LTF of the origin and target working point. The increment is corrected by the same coefficients as STF control(k_n ,k_i). Just as STF Neg, if d_{TPS} is less than the calibration data (d_{TPS} is negative), STF Neg is triggered. There is also coefficient k_d, to correct the LTF decay.

$$t_{lp\_rt} = t_{lp\_f} + (t_{lb\_t} - t_{lb\_o})\ k_n\ k_i, \tag{16}$$

$$t_{ln\_rt} = t_{ln\_f} + (t_{lb\_t} - t_{lb\_o})\ k_n\ k_i\ k_d, \tag{17}$$

where t_{lp_rt}—Real-time pulse width of positive LTF,
t_{lp_f}—Filtered pulse width of positive LTF,
t_{lb_t}—Basic initial pulse width of target working point of LTF,
t_{lb_o}—Basic initial pulse width of original working point of LTF,
t_{ln_rt}—Real-time pulse width of negative LTF,
t_{ln_f}—Filtered pulse width of negative LTF.

3.1.2.3 Transient fuel decay

There are four fuel decay coefficients corresponding to STF Pos, STF Neg, LTF Pos and LTF Neg. Take STF Pos for an example, if STF is triggered, a fuel step with correction named Δt_{sp_b} occurs, which is shown in Eq. (18):

$$\Delta t_{sp\_b}=(t_{sb\_t} - t_{sb\_o})\ k_n\ k_i, \tag{18}$$

where Δt_{sp_b}—Positive STF difference between target and original engine working point,
t_{sb_t}—Basic STF of target working point,
t_{sb_t}—Basic STF of original working point.

The LTF correction fuel decays from Δt_{sp_b} to zero step by step. The filter coefficient k'_{sp_d} is determined by p and n_e. There is another separate T_c coefficient k'_{sp_d} to compose the overall STF Pos decay coefficient k_{sp_d}. t_{sp_rt} is the output of LTF Pos calculation model and the t_{sp_f} is the output of STF Pos decay model. They are calculated alternatively. The output of the LTF Pos decay model is shown in Eqs. (19) and (20). As for the other three transient control items (STF Neg, LTF Pos and LTF Neg), the fuel decay complies with the same rule as STF Pos.

$$t_{sp\_f} = t_{sp\_rt} - t_{sp\_rt}\ k_{sp\_d}, \tag{19}$$

$$k_{sp\_d} = k_{c\_d} k'_{sp\_d}, \tag{20}$$

where k_{sp_d}—Positive STF decay coefficient,
k_{c_d}—Coefficient for STF and LTF which is influenced by coolant temperature,
k'_{sp_d}—Positive STF decay coefficient which is influenced by p and n_e .

Combining STF, LTF, V_b fuel and steady fuel correction with Eq. (9), the final output FPW t_f is calculated according to Eq. (21):

$$t_f = t_s(1+k_w)\ k_{WOT} + t_b + t_t + t_{sp\_rt} - t_{sn\_rt} + t_{lp\_rt} - t_{ln\_rt}, \tag{21}$$

3.2 Air path

The in-cylinder air mass flow rate is closely related with the combusted fuel. It has great influence on the engine torque. The fuel mass is calculated according to the "speed-density" principle. The air mass flow rate is influenced by n_e, η_v, p, V_h and T_i [32] . The air mass flow rate can be described as

$$q_a = V_h\ \eta_v\ p\ n_e\ /\ (120RT_i). \tag{22}$$

Hendricks derived η_v with empirical equation, which is shown in [33]

$$\eta_v p = \frac{1}{1+\Delta T_i/T_i}\left\{\left[\frac{(\kappa-1)(r-1)\iota+r}{\kappa(r-1)} - \frac{\kappa-1}{\kappa}\frac{T_{ov}}{T_i}\frac{m_{ov}}{\rho_m V_h}\right]p - \frac{p_e}{\kappa(r-1)}\right\} = S_i \cdot p_m - y_i, \tag{23}$$

$$\iota = \frac{1}{PV_h}\int_{io}^{ic} p\mathrm{d}V, \tag{24}$$

where ΔT_i—T_i change during intake stroke,
κ—Adiabatic exponent,
r—Compression ratio,
T_{ov}—Cylinder mixture average temperature at valve overlap,
m_{ov}—Cylinder mixture mass loss at valve overlap,
p_e—Exhaust background pressure,
io—Intake valve open,
ic—Intake valve close.

It is assumed that the parameters are estimated as follows: ΔT_i =15 K，T_i=300 K，r=10，p_e=105 kPa, ι=0.9, T_{ov}=1 000 K. The ratio of air mass loss to cylinder volume is 5%。So $S_i \approx 0.952$，$p_i \approx 0.079\ 3$。 Eq. (24) can be simplified into

$$\eta_v p = 0.952p - 0.097\ 3. \tag{25}$$

It can be seen from Eq. (25) that $\eta_v p$ is only related to p, and the error is less than 6% [33]. The empirical equation of η_v is deduced by means of this approach. In this paper, we add another parameter to correct the air mass flow rate, which is shown in Fig. 5. It represents the air mass loss between senor and in-cylinder.

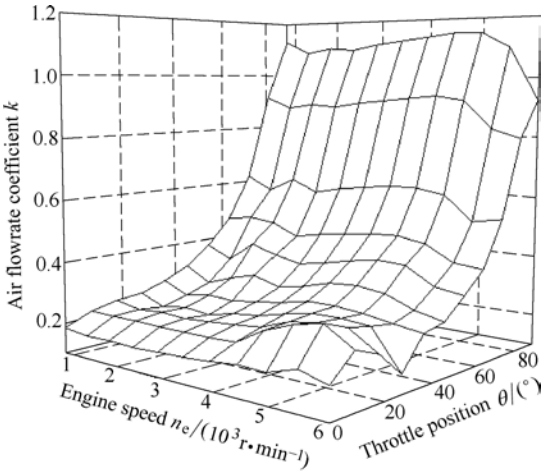

Fig. 5 Airflow coefficient

4 Simulation and Test Results

4.1 Model inputs

The model must be validated before it is put into practical application. We adopted the logged engine acceleration process of the urban part of New European Diving Cycle(NEDC). As shown in Fig. 6 and Fig. 7, all the signals come from real road test. The three accelerations correspond to vehicle launch and twice gear-changes.

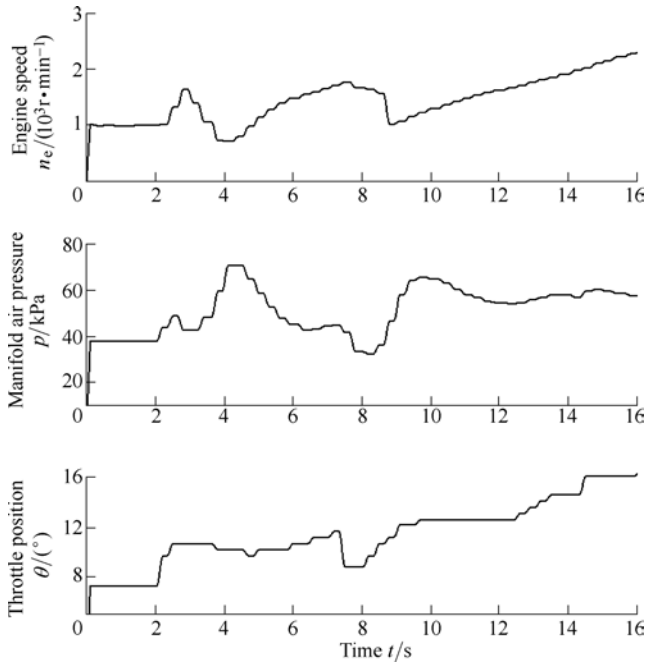

Fig. 6. n_e, p and θ

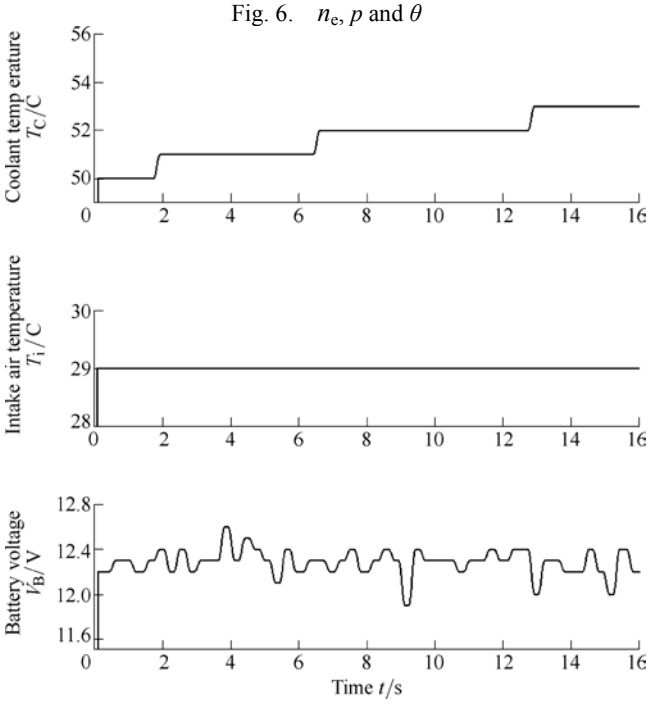

Fig. 7. T_c, T_i and V_b

The key signals related to fuel path include n_e, p, θ, T_c, T_i and V_b. n_e and p present the engine working point and determine the basic steady fuel. The θ signal is used for d_{TPS} calculation and further for STF control. It is also used for air mass flow coefficient determination. The T_i signal is related with steady fuel correction. It can be regard as constant within short time. The V_b fuel is used to compensate the steady fuel to ensure the effective injected fuel. The V_b fuel almost remains constant because of little voltage fluctuation. The engine experiences warm-up that the T_c increases from 50℃ to 54℃.

4.2 Fuel path

4.2.1 Steady fuel

The items related to basic steady fuel are shown in Fig. 8. The ideal fuel is calculated according to ideal gas equation without η_v and any other steady fuel correction. It is defined as

$$t_i = t_s/\eta_v = \eta_i\, pV_h/(14.7qT_i), \tag{26}$$

where t_i—Steady fuel calculated according to ideal gas equation,
t_s—Actual steady fuel.

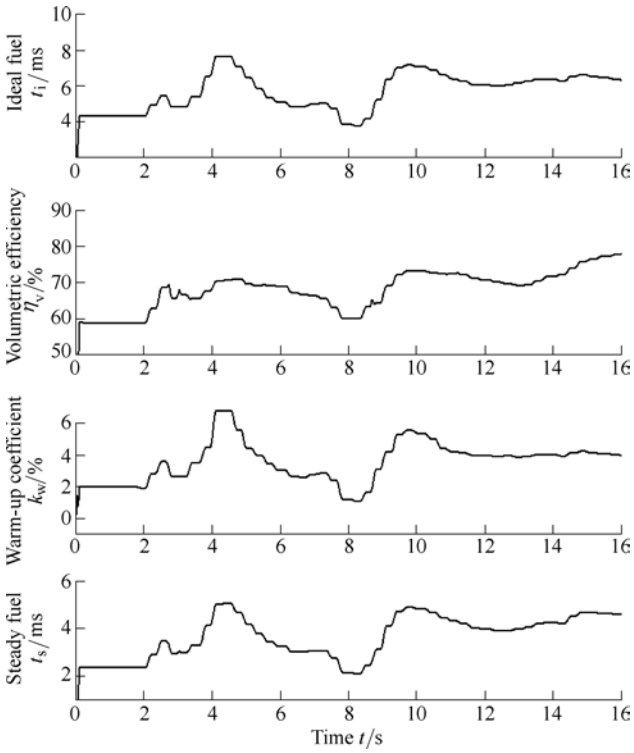

Fig. 8. Steady fuel: t_i, η_v, k_w, t_s

η_v is the most important parameter which is tested on bench. It is influenced by intake and exhaust system, valve train and engine working points. From the perspective of control strategy, η_v is influenced by n_e and p and it acts as the indicator of basic steady fuel. Except at some specific speed, η_v increases with n_e or p increasing as a whole. As can be seen in Fig. 8, η_v almost follows the trend of p, ranging from 60% to 80%.

The warm-up fuel is monotone increasing with p or T_c increasing. Because T_c is around 50 ℃, the trend of warm-up coefficient is closely similar to p. The fourth subplot of Fig. 8 is the steady fuel. It equals the ideal fuel corrected by η_v, warm-up fuel and WOT coefficients (Because the θ does not exceed the threshold, the WOT fuel is not activated).

4.2.2 Short-term fuel

Fig. 9 shows the parameters related with STF control. d_{TPS} is used as STF trigger and takes part in p_p calculation. It is a signed signal. d_{TPS} noise must be filtered before STF trigger check operation. As mentioned in section 2, there are two entrances for STF Pos: d_{TPS} and Δp_p. Both of them must be set reasonably not only to ensure reliable trigger but also to avoid signal noise disturbance. If d_{TPS} exceeds 1 degree and Δt_{lb} is positive, STF Pos is triggered. If d_{TPS} exceeds the negative threshold of −1 degree and Δt_{lb} is negative, STF Neg is triggered. As it can be seen in Fig. 9, STF Pos is triggered at 2.1 s. STF Neg is triggered at 7.45 s. Other d_{TPS} changes can be regarded as noise and have been filtered. The third and fourth subplots show the test (STFPosTest) and simulation(STFPosSimu) results of STF fuel control. The trigger time and amplitude match well.

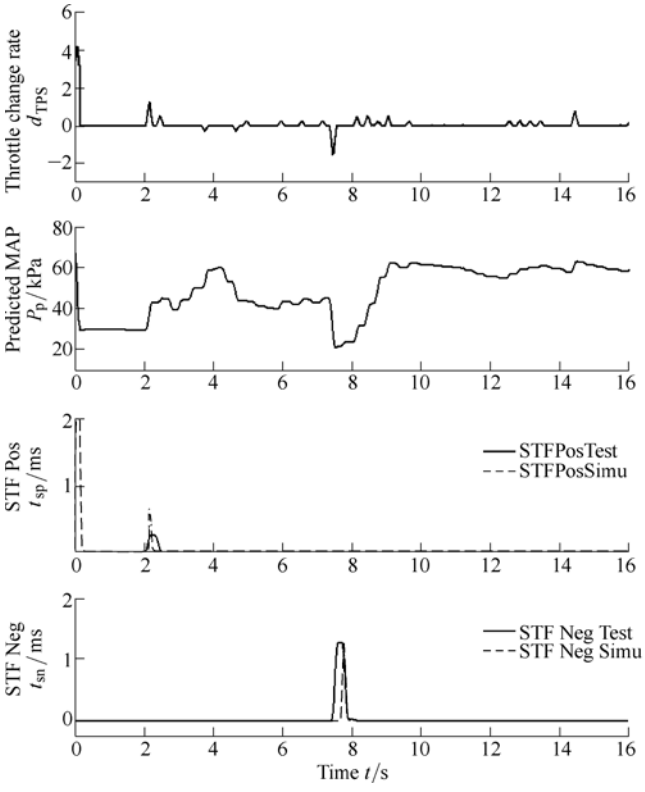

Fig. 9. STF fuel: d_{TPS}, p_p, STF fuel comparison

For STF Pos, an obvious difference occurs at time 0 s of STFPosSimu. It results from the simulation requirement of MATLAB/Simulink. d_{TPS} and p_p are initialized to zero at the beginning. This abnormal occurrence can be ignored.

The average error of STF Pos and STF Neg is 0.03 ms and 0.14 ms respectively, and the maximum error of them is 0.25 ms and 0.13 ms(The former abnormal error at the beginning of simulation is ignored).

4.2.3 Long-term fuel

Parameters related with LTF fuel control are shown in Fig. 10. The noise of d_p also must be filtered to avoid frequent LTF activation. If the d_p exceeds 1.6 kPa and Δt_{lb} is positive, LTF Pos is triggered. Compared with STF Pos, LTF Pos occurs more frequently and lasts longer because p changes more easily and more slowly. If d_p exceeds 1.6 kPa and Δt_{lb} is negative, LTF Neg is triggered. As can be seen in Fig. 10, the simulation results and test data of LTF control match well. The average error of LTF Pos and LTF Neg is 0.31 ms and 0.04 ms respectively, and the maximum error of them is 1.22 ms and 0.24 ms.

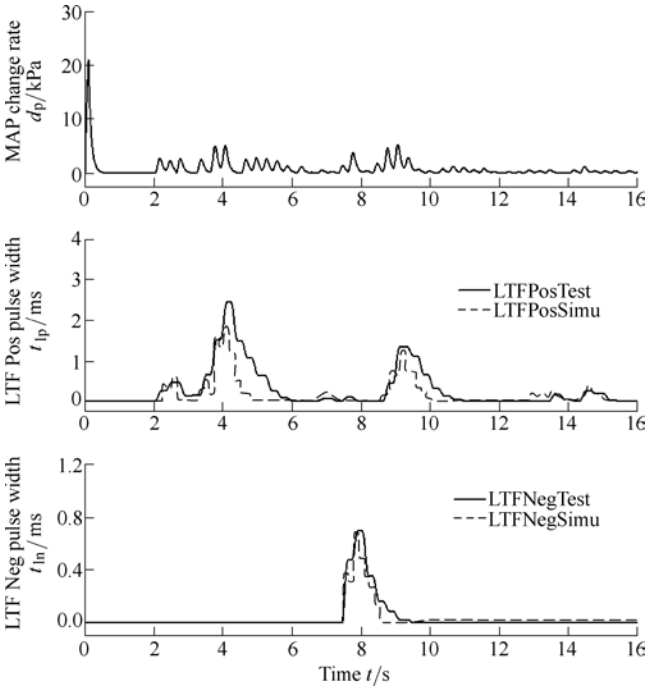

Fig. 10. LTF fuel: d_p, LTF fuel comparison

4.2.4 Fuel pulse width comparison

Fig. 11 shows the FPW comparison between simulation and test. The accuracy of steady fuel is firstly ensured. On the basis of validation of the four parts of transient fuel, the simulated FPW fits the data very well except for calculation at time 0 s. The error of time 0 s results from the difference between the simulation calculation mode and the logged data. The related signals are initialized to zero and lead to the simulated FPW(FuelSimu) being zero. But FuelSimu traces the tested FPW(FuelTest) at the second simulation step. Similar phenomenon appears at STF, LTF and steady fuel. The average error of FPW is 0.57 ms. The maximum error of them is 2 ms and it only occurs under engine heavy acceleration condition. (The former abnormal error at the beginning of simulation is ignored.)

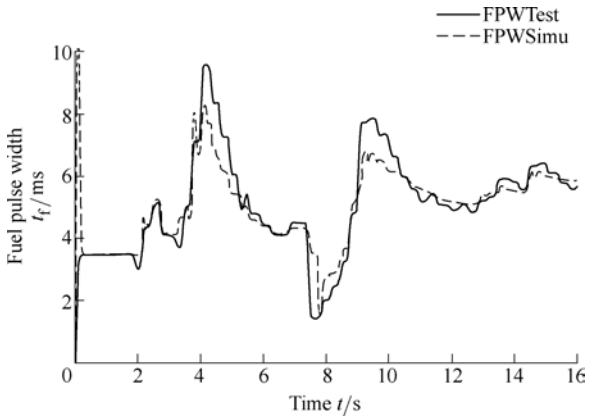

Fig. 11. LTF fuel: FPW comparison of simulation vs. test

4.3 Air mass flow and AFR validation

Besides the FPW, the AFR is another important indicator. It is very complicated because it is influenced by many factors such as valve train design, intake manifold, air mass calculation, transient fuel control, fuel film evaporation, residual gas and so on. We estimated the AFR with air and fuel path model merely from the perspective of mass flow. The AFR comparison between test and simulation is shown in Fig. 12. The FPW here is transferred into mass flow which is measured with g/s. The simulation and test AFR are shown in the third and fourth subplot of Fig. 12. For both of them, the AFR fluctuates around stoichiometric value(14.7). The influence of transient fuel is presented. The simulation and test data match well as a whole. Attention must be paid to AFR at time 7.8 s. There is much deviation between the simulation and the test. For the real-road test, the vehicle experiences sudden accelerator pedal releases at time 7.8 s. So the throttle experiences sudden close. The engine operates at "deceleration fuel cut-off" mode. The air mass flow rate cannot be calculated accurately and thus leads to the AFR deviation.

5 Conclusions

(1) According to the fuel wetting theory, the popular fuel compensation strategy is deduced into STF and LTF control to balance the fuel film deposit-evaporation. STF is to compensate the drastic fuel film loss to ensure adequate fuel into cylinder. STF is to compensate the mild fuel film loss continuously to ensure smooth AFR transition to steady state.

(2) The transient fuel control is application-oriented. Besides, the steady fuel is calculated according to the ideal gas equation, and the transient fuel model is also developed. The respective trigger condition, compensation strategy, and decay control of STF and LTF are determined.

(3) The transient fuel control strategy has been put into practice on ECU control. The engine acceleration is tested on a conventional vehicle platform. STF and LTF control are realized reliably.

(4) In order to validate the transient fuel control, the air-fuel ratio model is developed, which includes steady fuel model, transient fuel model and air mass model. The air-fuel ratio model adopts the same inputs as the engine acceleration test. The result shows that the maximum STF Pos, STF Neg, LTF Pos, LTF Neg and FPW error reach 0.03 ms, 0.14 ms, 0.31 ms, 0.04 ms and 2ms respectively. The average STF Pos, STF Neg, LTF Pos, LTF Neg and FPW are 0.25 ms, 0.13 ms, 1.22 ms, 0.24 ms and 0.82 ms respectively. For STF and LTF, a good agreement is found between the simulation curves and experimental curves as well.

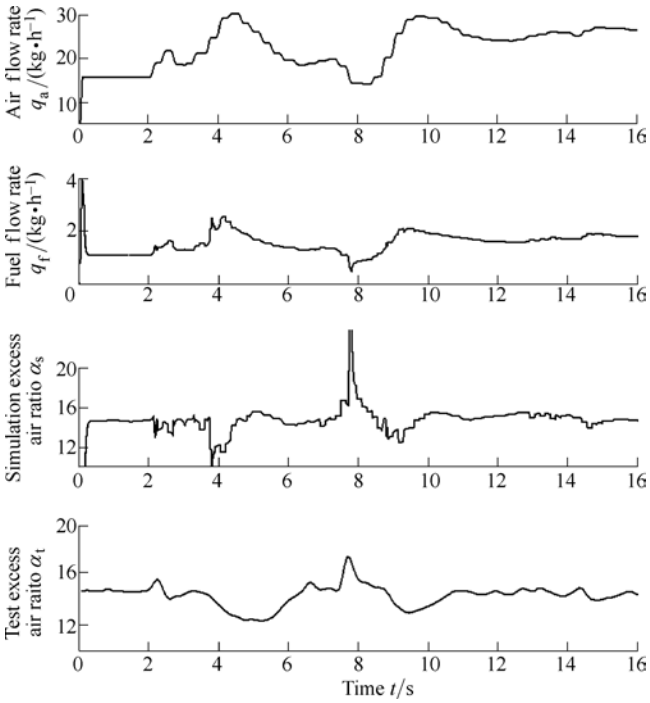

Fig. 12. AFR of simulation vs. test

References

[1] SHA Chaoqun. *The study and application research of motorcycle electronic control system*[D]. Beijing: Beijing Institute of Technology, 2002. (in Chinese)

[2] WANG Feng, MAO Xiaojian, YANG Lin, et al. Steady-state and idle optimization of internal combustion engine control strategies for hybrid electric vehicle[J]. *Chinese Journal of Mechanical Engineering*, 2008, 21(2): 58–64.

[3] HENDRICKS E, SORENSON S C. Mean value modeling of spark ignition engines[G]. *SAE Paper,* 900616, 1990.

[4] CHO H, MIN K, HWANG S, et al. Prediction of the air-fuel ratio in transient conditions using a model of liquid fuel behavior in the intake port of a spark-ignition engine[J]. *Proceedings of the Institution of Mechanical Engineers, Part D: Journal of Automobile Engineering*, 2000, 214(7): 731–740.

[5] TANG X G, JOSEPH R A, GARTH M M, et al. Optimal A/F ratio estimation model (synthetic UEGO) for SI engine cold transient AFR feedback control[G]. *SAE Paper,* 980798, 1998.

[6] WANG Cunlei, YIN Chengliang, LUO Gang, et al. Start and acceleration optimization of a parallel hybrid electric vehicle[J]. *Proceedings of the Institution of Mechanical Engineers, Part D: Journal of Automobile Engineering*, 2011, 225(5): 591–607.

[7] KARTHIKEYAN G, RAMAJAYAM M, PANNIRSELVAM A. Simulation of suction process of port fuel injection S.I. engine[J]. *International Journal of Applied Engineering Research*, 2011, 16(19): 2285–2295.

[8] ORLOV Y, KOLMANOVSKY I V, GOMEZ O. Adaptive identification of linear time-delay systems: from theory toward

application to engine transient fuel identification[J]. *International Journal of Adaptive Control and Signal Processing*, 2009, 23(2): 150–165.

[9] SUBRAMANIAN S S, RAJAMANI P, MANICKAM M. Study on the transient response of a fuel-injected (FI) motorcycle engine[G]. *SAE Small Engine Technology Conference,* 2010–32–0008, 2010.

[10] ZOU Bowen. *Research on model-based gasoline engine air-fuel ratio control technology*[D]. Hangzhou: Zhejiang University, 2006. (in Chinese)

[11] ZHONG Xianglin. *Study on control of MPI gasoline engine in transient condition based on fuel film model*[D]. Jilin University, 2007. (in Chinese)

[12] PRINCE S P. Development of a transient air fuel controller for an internal combustion engine[C]//*Proceedings of the IEEE International Conference on Systems, Man and Cybernetics, vol.4*, Vancouver BC, Canada, October 22–25, 1995: 3766–3771.

[13] LENZ U, SCHROEDER D. Transient air-fuel ratio control using artificial intelligence[G]. *SAT Paper,* 970618, 1997.

[14] TENG Qin, GONG Xiang, AN Peng. Adaptive prediction of transient air fuel ratio based on forgetting factor algorithm for a coal-bed gas engine[C]//*International Conference on Mechanical and Electronics Engineering*, Hefei, China, September 23–25, 2011: 814–819.

[15] HOU Zhixiang, WU Yihu. The research on air fuel ratio predictive model of gasoline engine during transient condition[C]// *International Conference on Mechatronics and Automation*, Harbin, China, August 5–8, 2007: 932–936.

[16] SHAYLER P J, GOODMAN M S, MA T. Transient air/fuel ratio control of an S.I. engine using neural networks[G]. *SAE Paper* 960326, 1996.

[17] HOU Zhixiang, SEN Quntai, WU Yihu. Air fuel ratio identification of gasoline engine during transient conditions based on Elman neural networks[C]//*Sixth International Conference on Intelligent Systems Design and Applications*, Jinan, China, October 16–18, 2006: 32–36.

[18] ZHANG Yanhong, XI Lifeng, Liu J. Transient air-fuel ratio estimation in spark ignition engine using recurrent neural network[C]//*11th International Conference on Knowledge-Based Intelligent Information and International Conference on Knowledge-Based Intelligent Information and Engineering Systems(KES 2007); Italian Workshop on Neural Networks,* Santiago de Compostela, Italy, September 12–14, 2007: 240–246.

[19] YAO Jubiao. Research on transient air fuel ratio control of gasoline engine[C]//*International Forum on Information Technology and Applications(IFITA 2009), Vol.3*, Chengdu, China, May 15–17, 2009: 610–613.

[20] ZHANG Cuiping, YANG Qingfo. Study on injection and ignition control of gasoline engine based on BP neural network[J]. *Chinese Journal of Mechanical Engineering*, 2003, 16(4): 441–444.

[21] WANG Ting, LIN Xuedong, FENG Xianzhen, et al. Research in fuel injection revision control of gasoline engine based on the electronic throttle during transient condition[C]//*2010 International Conference on Computer, Mechatronics, Control and Electronic Engineering*, Changchun, China, August 24–26, 2010: 285–287.

[22] LIU Zhiqiang, ZHOU Yucai. A fuzzy neural network and application to air-fuel ratio control under gasoline engine transient condition[C]// *2010 International Conference on Intelligent System Design and Engineering Application,* Changsha, China, 2010: 24–26.

[23] HAMILTON L J, COWART J S. Cold Engine transient fuel control experiments in a port fuel injected CFR engine[J]. *Journal of Engineering for Gas Turbines and Power*, 2008, 130(3): 291–299.

[24] ARREGLE J, BERMUDEZ V, SERRANO JR, et al. Procedure for engine transient cycle emissions testing in real time[J]. *Experimental Thermal and Fluid Science*, 2006, 30(5): 485–496.

[25] PENG Meicun, LIANG Xiaofeng, XU Chaomin. Control strategy & calibration of fuel film compensation in the transient conditions[C]// *International Conference on Energy, Environment and Sustainable Development(ICEESD)*, Shanghai, China, October 21–23, 2011: 2593–2598.

[26] PRUCKA R G, FILIPI Z S, HAGENA J R, et al. Cycle-by-cycle air-to-fuel ratio calculation during transient engine operation using fast response CO and CO_2 sensors[C]//*ASME Internal Combustion Engine Division fall technical conference*, Vancouver, Canada, September 23–26, 2012: 303–311.

[27] GAO Ying, FANG Yonglei, LI Jun, et al. Study on effect of fuel switch process on transient emissions for LPG engine[C]//*2011 International Conference on Electric Information and Control Engineering*, Wuhan, China, April 15–17, 2011: 5 384–5 387. (in Chinese)

[28] Throttle movement rate effects on transient fuel compensation in a port- fuel-injected si engine[G] *SAE Paper,* 2000-01-1937, 2000.

[29] AQUINO C F. Transient A/F control characteristics of a 5 liter central fuel injection engine[G]. *SAE Paper,* 810494, 1981.

[30] FOZO S R, AQUINO C F. Transient A/F characteristics for cold operation of a 1.6 liter engine with sequential fuel injection[G]. *SAE Paper,* 880961, 1988.

[31] LI Guoyong. *Intelligent control and MATLAB application in the electrically controlled engine*[M]. Beijing: Publishing House of Electronics Industry, 2007. (in Chinese)

[32] SUN Lei, WU Hao, HUANG Haiyan. A mean value model for gasoline engine and its usage in hardware-in-the-loop simulation[J]. *Vehicle Engine*, 2002(4): 27–29. (in Chinese)

[33] HENDRICKS E, CHEVALIER A, JENSEN M, et al. Modeling of the intake manifold filling dynamics[G]. *SAE Paper,* 960037, 1996.

Biographical notes

WANG Cunlei, born in 1981, is currently a postdoctoral researcher at *National Engineering Laboratory for Automotive Electronic Control Technology, Shanghai Jiao Tong University, China*. He received his PhD degree from *Shanghai Jiao Tong University, China*, in 2012. His research interests include automotive engine electronics and hybrid electric vehicle powertrain control

Tel: +86-13818767571; E-mail: clwang@sjtu.edu.cn

ZHANG Jianlong, born in 1976, is currently an assistant researcher at *National Engineering Laboratory for Automotive Electronic Control Technology, Shanghai Jiao Tong University, China*. He received his PhD degree on vehicle engineering at *Shanghai Jiao Tong University, China*, in 2006.

E-mail: zjlong@sjtu.edu.cn

YIN Chengliang, born in 1965, is currently a professor and a PhD candidate supervisor at *National Engineering Laboratory for Automotive Electronic Control Technology, Shanghai Jiao Tong University, China*. His main research interests include hybrid electric vehicle development.

E-mail: clyin1965@sjtu.edu.cn